Chaotic Modeling and Simulation (CMSIM) 4: 441-455, 2017

Cosmological Parameters and Higgs Boson in a Fractal Quantum System

Valeriy S. Abramov

Donetsk Institute for Physics and Engineering named after A.A. Galkin, Ukraine
(E-mail: vsabramov@mail.ru)

Abstract. The stochastic deformation and stress fields inside the fractal quantum system are investigated. It is shown that in the coupled system (dislocation – quantum dots) the presence of fractal quantum dot leads to a curvature of fractal dislocation core. For the fractal model of the Universe the relations of cosmological parameters and the Higgs boson are established. Estimates of the critical density, the expansion and speed-up parameters of the Universe (the Hubble constant and the cosmological redshift); temperature and anisotropy of the cosmic microwave background radiation were performed.
Keywords: Fractal Quantum System, Stochastic Deformation and Stress Fields, Higgs Boson, Cosmological Parameters, Fractal Model of the Universe.

1 Introduction

The development of the technique of spatial scanning made it possible to determine the speed of expansion of the Universe, the cosmic distances to the far Galaxies with great accuracy. This resulted to the discovery of the accelerated expansion of the Universe (Riess [1]). The latest achievements of the Universe researches were discussed at STARMUS-2016 [2]. Based on the analysis of supernovas burst of type la, a new value of the Hubble constant H_{01} (Riess [3]) is determined. In [3], possible reasons for the accelerated expansion of the Universe are discussed because of the presence: of zero energy and vacuum pressure (dark energy); an unknown dynamic field (possibly the Higgs field, Higgs [4]). Possible reasons for the anisotropic expansion of the Universe, the nature of the dark energy, the anisotropy of the cosmic microwave background (CMB) radiation were discussed in (Greene [5]). Large-scale structures of the Universe (voids and superclusters of Galaxies) form a "cosmic net" and influence on the temperature of the CMB radiation. In this case, relic photons passing through voids are colder in comparison with relic photons that pass through superclusters of Galaxies. Information on collisions of supermassive black holes at early stages of the formation of the Universe can retain relic radiation (Penrose [6]). At the same time, the appearance of ring structures may appear on the cosmic microwave background map of the Universe. After the merger of two black holes (Hawking [7]), the radiation of gravitational waves is possible (Abbott [8]). The hypothesis of the hierarchical

Received: 25 June 2017 / Accepted: 10 October 2017

ISSN 2241-0503

structure of the Universe became the basis for fractal cosmology. As separate elements of large-scale fractal structures, Galaxies, clusters and superclusters of Galaxies, the largest supercluster – Great Attractor, walls, filaments, voids are considered (Novosyadlyy [9]). Nanoscale fractal structures (based on the theory of fractional calculus) have been studied in [10-14]. In (Abramov [10, 11]), the parameters of the Higgs boson and the vortex-antivortex pair in a fractal quantum system are established. Quantum points, attractors, and the behavior of the deformation field of coupled fractal multilayer nanosystems have been investigated in (Abramov [12], Abramova [13, 14]). When creating a fractal model of the Universe, these models for fractal dislocations, quantum dots can be used as separate elements in modeling the deformation field of relic radiation and supernovas burst.

The aim of the work is to establish the connections of some cosmological parameters and the Higgs boson, to simulate the deformation field of the coupled fractal system (dislocation - quantum dot) within the framework of the fractal model of the Universe.

2 The Hubble constant and the Higgs boson

One of the main cosmological parameters is the Hubble constant H_0 in the Hubble law [1, 3]

$$\upsilon = H_0 r \ , \quad \text{or} \quad cz = H_0 r \ , \tag{1}$$

where υ is the speed of the Galaxy, r is the distance to it, c is the speed of light, z is the redshift. From this law follows the phenomenon of expansion of the Universe (metric expansion of space), which is experimentally confirmed on the scale of the cluster of Galaxies. In the early cosmological models it was assumed that the expansion of the Universe slows down, that is, the Hubble constant H_0 decreases. Measured by Cepheids (not using redshifts), the values of the Hubble constant and velocity were assumed to be equal to $H_0 = H_{02} = \upsilon_{02} / L_0 = 70.415674\,\mathrm{km \cdot s^{-1} \cdot Mpc^{-1}} = 2.282 \cdot 10^{-18}\,\mathrm{Hz}$, $\upsilon = \upsilon_{02} = 7.0415674 \cdot 10^6\,\mathrm{cm \cdot s^{-1}}$. Here $L_0 = N_a r_0 = 0.30857 \cdot 10^{25}\,\mathrm{cm}$; Avogadro number is $N_a = 6.025438 \cdot 10^{23}$; $r_0 = 10^6 l_0$, $l_0 = N_a^{-1}\mathrm{pc} = 51.2112149\,\mathrm{nm}$. However, the measurement of cosmic distances from supernovas burst of type 1a [1] in the expanding Universe and the agreement of these measurements with the data on redshift led to the discovery of the accelerated expansion of the Universe. According to the latest data [3] the Hubble constant is $H_0 = H_{01} = \upsilon_{01} / L_0 = 73.2\,\mathrm{km \cdot s^{-1} \cdot Mpc^{-1}} = 2.3722332 \cdot 10^{-18}\,\mathrm{Hz}$, speed is $\upsilon = \upsilon_{01} = 7.32 \cdot 10^6\,\mathrm{cm \cdot s^{-1}}$. Since $H_{01} > H_{02}$, it was concluded that there is an unknown energy with a negative pressure (dark energy), which is responsible for the accelerated expansion of the Universe. The characteristic distances $L_{02} = c_0 H_{02}^{-1}$, $L_{01} = c_0 H_{01}^{-1}$ are equal $L_{02} = 4.2574359\,\mathrm{Gpc}$, $L_{01} = 4.0954948\,\mathrm{Gpc}$, where c_0 is the limiting velocity of light in a vacuum. The distance L_{02} corresponds to the event horizon, and L_{01} is the distance to the supernova of type 1a. The characteristic frequencies are equal to $\nu_{a2}=N_a H_{02}=\upsilon_{02} r_0^{-1}=1.3750050\,\text{MHz}$, $\nu_{a1}=N_a H_{01}=\upsilon_{01} r_0^{-1}=1.4293744\,\text{MHz}$, and $\delta\nu_a=\nu_{a1}-\nu_{a2}=54.369458\,\text{kHz}$ is the frequency difference. The velocity difference $\upsilon_q=\upsilon_{01}-\upsilon_{02}=2.784326\cdot 10^5\,\text{cm}\cdot\text{s}^{-1}$ is close to the usual sound velocity in a condensed medium. The equations of connection for parallaxes $\varphi_{\eta 2}$, $\varphi_{\eta 1}$ [15] with characteristic distances L_{02}, L_{01} have the form

$$L_{02}L_0^{-1}=(\sin\varphi_{\eta 2})^{-1}=\eta_{02}=4257.4359\,;\quad L_{01}L_0^{-1}=(\sin\varphi_{\eta 1})^{-1}=\eta_{01}=4095.4948\,. \quad (2)$$

In our **model I** the main parameter is the parameter Q_{H0}, which is determined by expressions of the form

$$Q_{H0}=H_{01}/H_{02}=L_{02}/L_{01}=\eta_{02}/\eta_{01}=\sin\varphi_{\eta 1}/\sin\varphi_{\eta 2}\,. \quad (3)$$

Using the obtained numerical values, we find $Q_{H0}=1.039541282$. The declination angle θ_{H0} of the ecliptic axis to the equator can be determined from expressions

$$\sin^2\theta_{H0}=4(Q_{H0}-1)\,;\quad \cos^2\theta_{H0}=5-4Q_{H0}=\left|\sin\theta_{Ha}\right|\,;$$

$$b_{Ha}^2=\mathrm{tg}^2\theta_{Ha}\,;\quad \tau_{2H}^2-b_{Ha}^2=1\,;\quad \tau_{2H}=1+2\left|\xi_{Ha}\right|\,. \quad (4)$$

The relationships for b_{Ha} and τ_{2H} are obtained in [1, 3]. For **model I** the numerical values are $b_{Ha}=b_{0H}=1.559718408$; $\left|\xi_{Ha}\right|^2=\left|\xi_{0H}\right|^2=0.181800122$; $\theta_{H0}=23.43446018^\circ$. Value $b_{0H}>1$ [10, 11] indicates at the presence of condensates of effective atoms and Higgs bosons. By analogy with [10, 11] we introduce a quasi-one-dimensional lattice with two atoms in a unit cell (such as an effective atom and a Higgs boson with rest masses m_H and M_{H0}). The basic relationships of parameter $\left|\xi_{0H}\right|^2$ with the rest masses m_H and M_{H0} are

$$\left|\xi_{0H}\right|^2=m_H/M_{H0}=M_H/m_{H0}=E_H/E_{H0}=R_H/R_{H0}\,;\quad M_{Ha}=N_a M_H\,;$$

$$M'_{H0}=N_a m_{H0}\,;\quad R_H=2GM_{Ha}/c_0^2\,;\quad R_{H0}=2GM'_{H0}/c_0^2\,. \quad (5)$$

Here $M_H=N_a m_H=24.41158758\,\text{g}$, $m_{H0}=N_a M_{H0}=134.2770693\,\text{g}$ and $E_H=22.73090194\,\text{GeV}$, $E_{H0}=125.03238\,\text{GeV}$ are molar masses and rest energies of an effective atom, the Higgs boson; $R_H=21.84067257\,\mu\text{m}$, $R_{H0}=120.1356321\,\mu\text{m}$ allow the interpretation of the Schwarzschild radii of black holes with masses M_{Ha}, M'_{H0}; $G=6.672\cdot 10^{-8}\text{cm}^3\text{g}^{-1}\text{s}^{-2}$ is gravitational Newtons constant. Based on (3) - (5) for calculating the frequency (type $\nu_{Hx} = \nu_{a1} S'_{Hx}$, $\nu'_{Hx} = \nu_{a2} S'_{Hx}$) and mass (of the type $N_{Hx} = N_0 S'_{Hx}$, where N_0 is the total number of effective atoms) spectra, taking into account the condensates of effective atoms and Higgs bosons by analogy with [10, 11], we find the parameters of the theory S'_{Hx} ($x = 1,2,3,4$)by the formulas

$$|S'_{H1}| = |S'_{01}| = (\sin^2 \theta_{H0}) / 4 = Q_{H0} - 1 ; \quad S'_{03} + |S'_{01}| = 0.5 ;$$
$$S'_{H2} = S'_{02} = ((2 - \cos^4 \theta_{H0})^{1/2} - 1) / 4 ; \quad S'_{04} - S'_{02} = 0.5 . \quad (6)$$

The numerical values of these parameters are $|S'_{01}| = 0.039541282$, $S'_{02} = 0.03409$, $S'_{03} = 0.460458718$, $S'_{04} = 0.53409$. From the calculated value $\sigma_H = \sin^4 \theta_{H0} = 0.025016208$ we find the densities distribution functions of the Bose (n_{B1}, n'_{B1}, n_{B2}, n'_{B2}), Fermi (n_{F1}, n'_{F1}) types

$$n_{B1} = 2\sigma_H / (1 - \sigma_H) ; \quad n'_{B1} - n_{B1} = 1 ; \quad n_{B2} = 1 / n_{B1} ; \quad n'_{B2} - n_{B2} = 1 ;$$
$$n_{F1} = 1 / (1 + n_{B2}) ; \quad n'_{F1} = 1 / (1 + n_{B1}) ; \quad n_{F1} + n'_{F1} = 1 . \quad (7)$$

In **model I** values of parameters are $n'_{F1} = 0.951188659$, $\Omega_{tH} = Q_{H0} + |S'_{H1}| = 1.079082564$, $\Omega_{b1} = |\xi_{0H}|^2 / 4 = 0.045450031$. They can be used as estimates of the sum ($\Omega_{d1} = n'_{F1}$) of densities (normalized to critical density) $\Omega_{d1} = \Omega_{\Lambda 1} + \Omega_{c1}$ of dark energy ($\Omega_{\Lambda 1} = 0.7255943$) and cold dark matter ($\Omega_{c1} = (n'_{F1} - n_{F1}) / 4 = 0.2255943$), the total density of the Universe (Ω_{tH}), ordinary baryons density of the matter (Ω_{b1}).

For **model II** the main parameter is the declination angle θ_{E0} of the ecliptic axis to the equator. By analogy with (3), (4) parameter Q_{E0} is determined from equations of the form

$$\sin^2 \theta_{E0} = 4(Q_{E0} - 1) ; \quad \cos^2 \theta_{E0} = 5 - 4Q_{E0} = |\sin \theta_{Ea}| ;$$
$$b^2_{Ea} = \mathrm{tg}^2 \theta_{Ea} ; \quad \tau^2_{2E} - b^2_{Ea} = 1 ; \quad \tau_{2E} = 1 + 2|\xi_{Ea}| ;$$
$$Q_{E0} = H_{E0} / H_{02} = L_{02} / L_{E0} = \eta_{02} / \eta_{E0} = \sin \varphi_{E0} / \sin \varphi_{\eta 2} . \quad (8)$$

From the known inclination angle of the ecliptic axis to the equator $\theta_{E0} = 23.43928108^\circ$ [15] from (8) we find parameters $Q_{E0} = 1.039556635$, $b_{Ea} = 1.559327942$, $|\xi_{Ea}|^2 = 0.18166$, $H_{E0} = 2.372268241 \cdot 10^{-18}\,\mathrm{Hz}$, $L_{E0} = 4.0954343\,\mathrm{Gpc}$. In this case the characteristics frequency, speed are $\nu_{E0} = N_a H_{Ea} = \upsilon_{E0} r_0^{-1} = 1.4293955\,\mathrm{MHz}$, $\upsilon_{E0} = 7.3201081 \cdot 10^6\,\mathrm{cm \cdot s^{-1}}$; differences are $\delta\nu_E = \nu_{E0} - \nu_{a2} = (\upsilon_{E0} - \upsilon_{02}) r_0^{-1} = 75.6454706\,\mathrm{kHz}$, $\upsilon_E = \upsilon_{E0} - \upsilon_{02} = 2.784326 \cdot 10^5\,\mathrm{cm \cdot s^{-1}}$. The calculated values of the Hubble constant H_{E0}, the distance L_{E0} to the supernova of the type Ia are close to those measured H_{01}, L_{01} [3] for the accelerated expansion of the Universe. Value $b_{Ea} > 1$ again indicates at the presence of condensates of effective atoms and Higgs bosons. We introduce a quasi-one-dimensional lattice with two atoms in an elementary cell (such as an effective atom and a Higgs boson with rest masses m_{Ea} and M_{H0}). The basic relationships of $|\xi_{Ea}|^2$ with m_{Ea} and M_{H0} are

$$|\xi_{Ea}|^2 = m_{Ea} / M_{H0} = M_{Ea} / m_{H0} = E_{Ea} / E_{H0} = R_{Ea} / R_{H0};$$
$$R_{Ea} = 2GM'_{Ea} / c_0^2; \quad M'_{Ea} = N_a M_{Ea}. \tag{9}$$

Here $M_{Ea} = N_a m_{Ea} = 24.3927724\,\mathrm{g}$ and $E_{Ea} = 22.71338215\,\mathrm{GeV}$ are molar mass and rest energy of an effective atom in **model II**; $R_{Ea} = 21.82383892\ \mu\mathrm{m}$ admits an interpretation as the Schwarzschild radius of a black hole with mass M'_{Ea}. To calculate the frequency (type $\nu_{Ex} = \nu_{E0} S'_{Ex}$) and mass (of the type $N_{Ex} = N_{E0} S'_{Ex}$, where N_{E0} is the total number of effective atoms) spectra, taking into account the condensates of effective atoms and Higgs bosons, we find the parameters of the theory S'_{Ex} ($x = 1, 2, 3, 4$) for **model II** by formulas

$$|S'_{E1}| = (\sin^2\theta_{E0}) / 4 = Q_{E0} - 1; \quad S'_{E3} + |S'_{E1}| = 0.5;$$
$$S'_{E2} = ((2 - \cos^4\theta_{E0})^{1/2} - 1) / 4; \quad S'_{E4} - S'_{E2} = 0.5. \tag{10}$$

The numerical values of these parameters are $|S'_{E1}| = 0.039556635$, $S'_{E2} = 0.034101373$, $S'_{E3} = 0.460443365$, $S'_{E4} = 0.534101373$. From the calculated value $\sigma_E = \sin^4\theta_{E0} = 0.025035638$ we find the densities distribution functions of the Bose ($n_{B3}, n'_{B3}, n_{B4}, n'_{B4}$), Fermi ($n_{F2}, n'_{F2}$) types

$$n_{B3} = 2\sigma_H / (1 - \sigma_H); \quad n'_{B3} - n_{B3} = 1; \quad n_{B4} = 1 / n_{B3}; \quad n'_{B4} - n_{B4} = 1;$$
$$n_{F2} = 1 / (1 + n_{B4}); \quad n'_{F2} = 1 / (1 + n_{B3}); \quad n_{F2} + n'_{F2} = 1. \tag{11}$$

Values are equal $n'_{F2} = 0.951151673$, $\Omega_{tE} = Q_{E0} + |S'_{E1}| = 1.07911327$, $\Omega_{b2} = |\xi_{Ea}|^2 / 4 = 0.045415$. Parameters $n'_{F2} = \Omega_{d2} = \Omega_{\Lambda 2} + \Omega_{c2}$, Ω_{t2}, Ω_{b2} allow interpretation as a sum of the densities of dark energy ($\Omega_{\Lambda 2} = 0.7255758$) and cold dark matter ($\Omega_{c2} = (n'_{F2} - n_{F2}) / 4 = 0.2255758$), the total density of the Universe, ordinary baryons density of the matter. They can be used as estimates of these parameters in **model II**.

The difference in the inclination angles of the ecliptic axes to the equator from **models II** and **I** is equal $\delta\theta_0 = \theta_{E0} - \theta_{H0} = 17.35524''$. This value is close to value $2\varphi_0$, where $\varphi_0 = 8.794148''$ is the parallax of the Sun [15]. Condition $\delta\theta_0 = 2\varphi_0$ makes it possible to combine **models I** and **II**.

3 Parameters of CMB radiation and Higgs boson

To describe the parameters of the CMB radiation (**model III**), we introduce random variables $\hat{x}''$, $(\hat{x}'')^+$, $\hat{y}''$, $(\hat{y}'')^+$, which are the sums of independent random variables $\hat{n}_{FH1}$, $\hat{n}_{FH2}$, $\hat{n}_{FG1}$, $\hat{n}_{FG2}$ (with binomial distribution laws)

$$\hat{x}'' = \sum_{i=1}^{N_a} \hat{n}_{FH1}\,; \quad (\hat{x}'')^+ = \sum_{i=1}^{N_a} \hat{n}_{FH2}\,; \quad \hat{n}_{FH1} = a_H^+ a_H\,; \quad \hat{n}_{FH2} = b_H^+ b_H\,;$$

$$\hat{y}'' = \sum_{i=1}^{N_a} \hat{n}_{FG1}\,; \quad (\hat{y}'')^+ = \sum_{i=1}^{N_a} \hat{n}_{FG2}\,; \quad \hat{n}_{FG1} = a_G^+ a_G\,; \quad \hat{n}_{FG2} = b_G^+ b_G\,. \quad (12)$$

Here for the description of elementary excitations (by analogy with the theory of semiconductors) for the operators of occupation numbers $a_H^+ a_H$, $b_H^+ b_H$, $a_G^+ a_G$, $b_G^+ b_G$ a "hole" representation is used. The expected values for these operators of Fermi type are determined by expressions

$$M(\hat{n}_{FH1}) = 1 - Q_H\,; M(\hat{n}_{FH2}) = Q_H\,; \; M(\hat{n}_{FG1}) = Q_G\,; M(\hat{n}_{FG2}) = 1 - Q_G\,, \quad (13)$$

Which are carried out at $Q_H \in [0;1]$, $Q_G \in [0;1]$. Symbols "+" and "M" mean the operations of hermitian conjugation and expected value. For $Q_H > 1$ operators of Fermi type $\hat{n}_{FH1}$, $\hat{n}_{FH2}$ are replaced by operators of Bose type $\hat{n}_{BH1} = c_H^+ c_H$, $\hat{n}_{BH2} = c_H c_H^+$ with expected values $M(\hat{n}_{BH1}) = Q_H - 1$; $M(\hat{n}_{BH2}) = Q_H$ .For the random variables $\hat{x}''$, $(\hat{x}'')^+$, $\hat{y}''$, $(\hat{y}'')^+$ we obtain

$$M(\hat{x}'') = N_a|1 - Q_H|\,; M((\hat{x}'')^+) = N_a Q_H\,; M(\hat{y}'') = N_a Q_G\,; M((\hat{y}'')^+) = N_a(1 - Q_G)\,. (14)$$

On the other hand, random variables $\hat{x}''$, $(\hat{x}'')^+$, $\hat{y}''$, $(\hat{y}'')^+$ are connected with one-dimensional random variables $\hat{x}'$, $(\hat{x}')^+$, $\hat{y}'$, $(\hat{y}')^+$, $\hat{x}$, $\hat{x}^+$, $\hat{y}$, $\hat{y}^+$ (each of which has two possible states) by the relations

$$\hat{x}'' = \hat{x}' / 2\nu_G\,; \quad \hat{x}' = \hat{x} - x_0 Q_H\,; \quad \hat{y}'' = \hat{y}' N_a / \nu_{r0}\,; \quad \hat{y}' = \hat{y} - y_0(1 - Q_G)\,;$$

$$(\hat{x}'')^+ = (\hat{x}')^+ / 2\nu_G\,; \quad (\hat{y}'')^+ = (\hat{y}')^+ N_a / \nu_{r0}\,. \quad (15)$$

Possible states for $\hat{x}$ and $\hat{y}$ are described by parameters x_0, ν_G and y_0, ν_{r0}, which are related to parameters of graviton and Higgs boson [11] by relations

$$E_G = M_G c_0^2 = \hbar 2\pi N_a \nu_G\,; \; M_G = N_a m_G\,; \; E_{H0} / E_G = M_{H0} / M_G = N_{HG}\,. \quad (16)$$

Here M_G, m_G are molar mass and rest mass of graviton; N_{HG}=1.0318305$\cdot 10^{16}$; E_G=12.11753067 μeV and $N_a \nu_G$=2.9304515 GHz, ν_G=4.8634664$\cdot 10^{-15}$ Hz are characteristic energy and frequencies for graviton. Applying the operation of expected value to (15), we find

$$M(\hat{x}) = x_0 Q_H + 2\nu_G N_a |1 - Q_H|\,; \quad M(\hat{x}') = 2\nu_G N_a |1 - Q_H|\,;$$

$$M(\hat{y}) = \nu_{r0} Q_G + y_0 (1 - Q_G)\,; \quad M(\hat{y}') = \nu_{r0} Q_G\,. \tag{17}$$

Taking into account the conditions for the equality of expected values $M(\hat{y}') = M(\hat{x}')$ from (17) and dispersions $D(\hat{y}') = D(\hat{x}')$, we find two equations for search eigenvalues ν_{r0}, ν_G, depending on parameters Q_H, Q_G

$$\nu_{r0} Q_G = 2\nu_G N_a \left|1 - Q_H\right|; \quad 2\nu_G N_a / (1 - Q_G) = \nu_{r0} Q_H \left|1 - Q_H\right|. \tag{18}$$

From equations (18) we find the basic nonlinear equations for functions Q_G, B_G, that depend on an arbitrary argument Q_H

$$Q_G = Q_H (1 - Q_H)^2 / (1 + Q_H (1 - Q_H)^2)\,; \quad B_G = 1 - 2Q_G\,. \tag{19}$$

Dependences of functions Q_G, B_G and derivatives $V_Q = dQ_G / dQ_H$, $A_Q = dV_Q / dQ_H$ on Q_H are given on fig. 1.

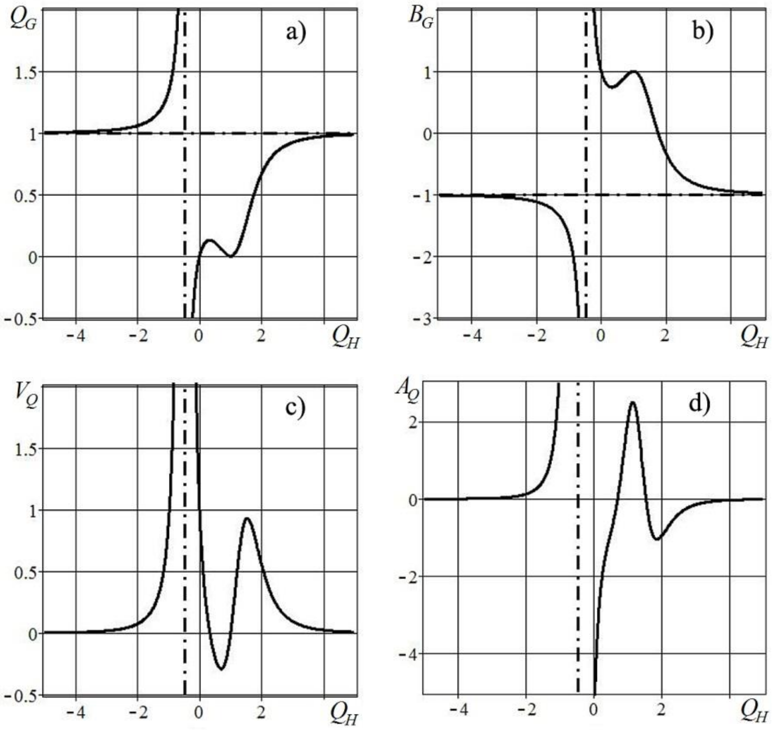

Fig. 1. The behavior of functions Q_G (a), B_G (b), V_Q (c), A_Q (d) on Q_H. Vertical and horizontal asymptotes are dashed dotted lines.

Indicated functions Q_G, B_G, V_Q admit representations

$$Q_G = Q_H (1 - Q_H)^2 / Q_0\,; \quad B_G = (Q_{H7} - Q_H)[(Q_H - Q'_{H8})^2 + (Q''_{H8})^2] / Q_0\,;$$

$$V_Q = 3(Q_H - Q_{H2})(Q_H - Q_{H4}) Q_0^{-2}\,; \quad Q_0 = (Q_H - Q_{H1})[(Q_H - Q'_{H5})^2 + (Q''_{H5})^2]\,. \tag{20}$$

Here $Q_{H1} = -0.465571232$; $Q_{H2} = 1/3$; $Q'_{H5} = \mathrm{Re}\, Q_{H5} = 1.232785616$, $Q''_{H5} = \mathrm{Im}\, Q_{H5} = 0.792551993$; $Q_{H4} = 1$; $Q'_{H8} = \mathrm{Re}\, Q_{H8} = 0.122561167$, $Q''_{H8} = \mathrm{Im}\, Q_{H8} = 0.744861767$ and $Q_{H7} = 1.754877667$ determine positions of the vertical asymptote (fig. 1 a, c, d); local maximum (fig. 1 a) or minimum (fig. 1 b); complex zeros of the function Q_0; local minimum (fig. 1 a) or maximum (fig. 1 b); complex and real zeros of function B_G (fig. 1 b). Values $Q_{H3} = 0.700790572$ and $Q_{H6} = 1.537746366$ determine positions of the inflection points for Q_G (fig. 1 a); local minimum and maximum for V_Q (fig. 1 c); zeros of the function A_Q (fig. 1 d). The horizontal asymptotes are defined by equations $Q_G = 1$ (fig. 1 a), $B_G = -1$ (fig. 1 b). Values $Q_{H9} = 1.150931347$ and $Q_{H10} = 1.863868407$ determine positions local maximum and minimum for function A_Q (fig. 1 d). Values of functions $Q_G(Q_H)$, $V_Q(Q_H)$, $A_Q(Q_H)$, $\nu_{r0}(Q_H)$, calculated for some values of Q_H ($Q_H < 1$ and $Q_H > 1$) for **models I** and **II** are given in table 1. When passing through the value $Q_H = 1$ function V_Q changes sign in both models (fig. 1 c, table 1), and function A_Q remains positive and increases (fig. 1 d, table 1).

Table 1. Numerical values of parameters for **models I** and **II**.

Parameters	**Model I**		**Model II**	
Q_H	$1/Q_{H0}$	Q_{H0}	$1/Q_{E0}$	Q_{E0}
Q_G	0.001389864	0.001622699	0.001390880	0.001623981
V_Q	-0.071534724	0.083501447	-0.071559680	0.083535470
A_Q	1.756606245	2.216025177	1.756510478	2.216099863
ν_{r0}, GHz	160.3988698	142.8161605	160.3415137	142.7588046

Variant $V_Q > 0$ and $A_Q > 0$ corresponds to the accelerated expansion of the Universe. At the same time, for **model I**, the calculated value of the frequency $\nu_{r0}(Q_{H0}^{-1})$ is near the maximum of the CMB radiation at frequency $160.4\,\mathrm{GHz}$, and the value $\nu_{r0}(Q_{H0})$ is shifted to the long-wave region (redshift effect). A similar redshift effect is observed for **model II** with shifted values of frequences $\nu_{r0}(Q_{E0}^{-1})$ and $\nu_{r0}(Q_{E0})$. To describe the anisotropy of the CMB radiation on the basis of [10, 11], we write the expressions (at $\delta N'_0 \neq 0$, $\Delta'_0 \neq 0$), relating temperatures T_A, T'_A [16] with the temperatures of the CMB radiation $T_r = 2.72548\,\mathrm{K}$, the phase transition T_{cH} [10, 11] and other spectral parameters

$$T_A = 2T_{cH} N_{H2}; \quad N_{H2} = N'_{02} S'_{H2} = N_0 S'_{02} = N_{E0} S'_{E2}; \quad 2\varepsilon_{01} / 2\varepsilon_{02} = (\xi'_0)^2;$$

$$N'_{02} = [(N'_0)^2 - (\delta N'_0)^2]^{1/2}; \quad N'_{01} = [(N'_0)^2 + (\delta N'_0)^2]^{1/2}; \quad N_{ra} = T_r / T_A;$$

$$2\varepsilon_{01} = 2[E_{H0}^2 + (\Delta'_0)^2]^{1/2}; \quad 2\varepsilon_{02} = 2[E_{H0}^2 - (\Delta'_0)^2]^{1/2}; \quad T'_A = T_r / z'_{A2};$$

$$z'_{A2} = T_r / (T_A + \delta T_A); z'_{A2} + z'_\mu = N_{ra}; \delta T_A = T'_A - T_A; 2\delta T_r = N_{ra} Q_{H3} \delta T_A. \quad (21)$$

On the basis of (21), the initial parameters $T_{cH} = 100.06602\,\text{nK}$, $S'_{H2} = 0.034978505$, $N'_0 = 3.73846796 \cdot 10^5$ [10, 11] for $\delta N'_0 = 0$, $\Delta'_0 = 0$ we find values $N_{H2} = 1.307835827 \cdot 10^4$, $T_A = 2.61739852\,\text{mK}$ [10, 11]; $T'_A = 2.635582153\,\text{mK}$; root-mean-square deviation of temperature $\delta T_A = 18.183633\,\mu\text{K}$; number of relic photons $N_{ra} / 2 = 520.6467375$; normal redshift $z'_{A2} = 1034.109294$; cosmological redshift $z'_\mu = 7.184181$; the temperature difference between the hot and cold regions of the CMB radiation (due to the presence at $Q_{H3} \neq 0$ of dipole anisotropy) $\delta T_r = 6.634559017\,\text{mK}$; Higgs field $2\varepsilon_{02} = 2E_{H0} = 2\varepsilon_{01}$. At $\delta N'_0 \neq 0$, $\Delta'_0 \neq 0$, we find the parameters (table 2) and the value $N_{H2} = 1.293903061 \cdot 10^4$. Temperatures $T_A = 2.589514592\,\text{mK}$, $T'_A = 2.607698225\text{mK}$ are shifted down at practically unchanged δT_A. The number of relic photons $N_{ra} / 2 = 526.2530685$, the usual redshift $z'_{A2} = 1045.16695$, the cosmological redshift $z'_\mu = 7.339187$, the temperature difference $\delta T_r = 6.706\,\text{mK}$ increase. The Higgs field $2\varepsilon_{02}$ decreases, and the energy of the two coupled Higgs bosons $2\varepsilon_{01}$ increases and at $\delta N'_0 = \delta N_0$ they become equal $2\varepsilon_{02} = 246.1873393\,\text{GeV}$, $2\varepsilon_{01} = 253.8829698\,\text{GeV}$.

Table 2. Numerical values of spectral parameters.

$\delta N'_0$ / Parameters	$\delta N'_0 = \delta N'_0$	$\delta N'_0 = \delta N_{E0}$	$\delta N'_0 = \delta N_0$
	$5.40854003 \cdot 10^4$	$6.48421997 \cdot 10^4$	$6.55788523 \cdot 10^4$
N'_{01}	$3.777388746 \cdot 10^5$	$3.794284356 \cdot 10^5$	$3.795550194 \cdot 10^5$
N'_{02}	$3.699137688 \cdot 10^5$	$3.681805481 \cdot 10^5$	$3.680500523 \cdot 10^5$
$\psi'_0 = \delta N'_0 / N'_0$	0.144672633	0.173445915	0.175416382
$(\xi'_0)^2 = N'_{01} / N'_{02}$	1.021153865	1.030549923	1.031259246
$\Delta'_0 = \psi'_0 E_{H0}$, GeV	18.08876362	21.68635559	21.93272771
$2\varepsilon_{01}$, GeV	252.6681572	253.7982984	253.8829698
$2\varepsilon_{02}$, GeV	247.4339724	246.2746274	246.1873393

4 Simulation of the deformation field of a coupled system: dislocation - quantum dot

Function $B_G(Q_H)$ from (19) and fig. 1 b is nonlinearly related to the dimensionless displacement function of the deformation field u in the fractal model of the Universe. The behavior of such deformation and stress fields is essentially stochastic. The deformation fields of the relic radiation and supernova bust are modeled by deformation fields of the fractal dislocation (the set of quantum dots with small radius) and the quantum dot (with an imaginary attractor), respectively. By analogy with [10, 11] the behavior of function u for the coupled system (fractal dislocation – fractal quantum dot) is first modelled by expressions for constant moduli $k_{\mathrm{i}} = 0.5$ of elliptic functions

$$u = \sum_{\mathrm{i}=1}^{2} R_{\mathrm{i}}(1-\alpha_{\mathrm{i}})B_{G\mathrm{i}} / Q_{\mathrm{i}} \ ; \qquad B_{G\mathrm{i}} = 1 - 2sn^2(u - u_{0\mathrm{i}}, k_{\mathrm{i}}) \ ;$$

$$Q_1 = p'_{11}n + p'_{21}m \ ; \quad Q_2 = p'_{02} - b_{12}(n - n_{02})^2 / n_{c2}^2 - b_{22}(m - m_{02})^2 / m_{c2}^2 \ . \qquad (22)$$

Simulation is performed on a discrete lattice $N_1 \times N_2 \times N_3$, whose nodes are given integers n, m, j ($n = \overline{1, N_1}$; $m = \overline{1, N_2}$; $j = \overline{1, N_3}$), $N_1 = 240$, $N_2 = 180$. Here $\alpha_{\mathrm{i}} = 0.5$ is the fractal dimension of the deformation field u along the Oz-axis ($\alpha_{\mathrm{i}} \in [0,1]$); $u_{0\mathrm{i}} = 29.537$ are the constant (critical) displacements. The simulation results are given in fig. 2.

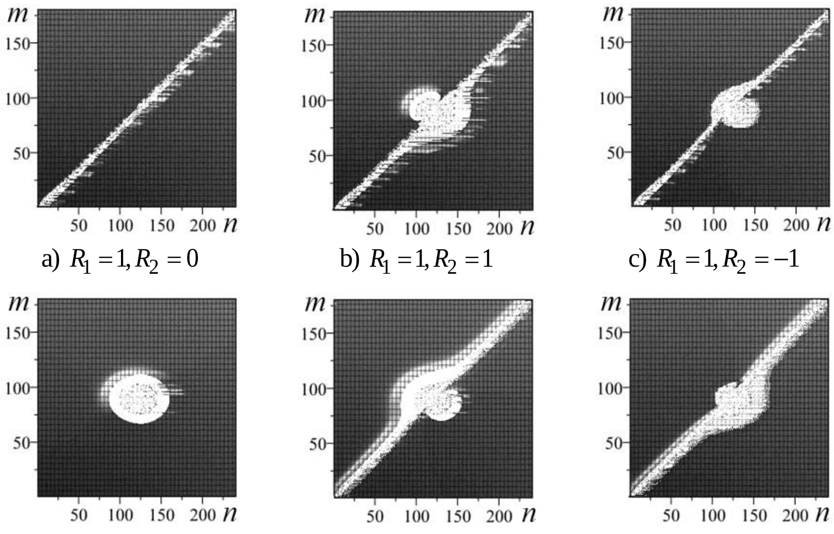

a) $R_1 = 1, R_2 = 0$ b) $R_1 = 1, R_2 = 1$ c) $R_1 = 1, R_2 = -1$

d) $R_1 = 0, R_2 = 1$ e) $R_1 = -1, R_2 = 1$ f) $R_1 = -1, R_2 = -1$

Fig. 2. Cross-sections $u \in [-0.5; 0.5]$ (top view) for dislocation (a), quantum dot (d), coupled system (b,c,e,f) with constant modules k_{i} .

The fractal dislocation ($\mathrm{i} = 1$) is described by parameters $p'_{11} = -0.0739$; $p'_{21} = 0.0975$.

The fractal quantum dot ($\mathrm{i} = 2$) is described by parameters $p'_{02} = -3.457 \cdot 10^{-11}$; $b_{12} = b_{22} = 1$; $n_{02} = 119.1471$; $m_{02} = 89.3267$; $n_{c2} = 44.4793$; $m_{c2} = 25.7295$.

Parameters R_{i} determine the orientation of the deformation fields of separate structures in the coupled system.

The displacement functions are real functions. Near the localization region of the fractal quantum dot, the curvature of fractal dislocation core is observed (fig. 2b,c,e,f).

The nature of this curvature depends on the mutual orientation of the deformation fields of the separate structures (fig. 2a,d) in the coupled system. With different orientations (fig. 2c,e), the shape of this curvature is convex; with the same orientation (fig. 2b,f) is concave.

When modelling early stages of the formation of the Universe or transient effects after a supernova bust of type la, we assume that the modules k_{i} are functions of the indices n , m , j of the bulk discrete lattice.

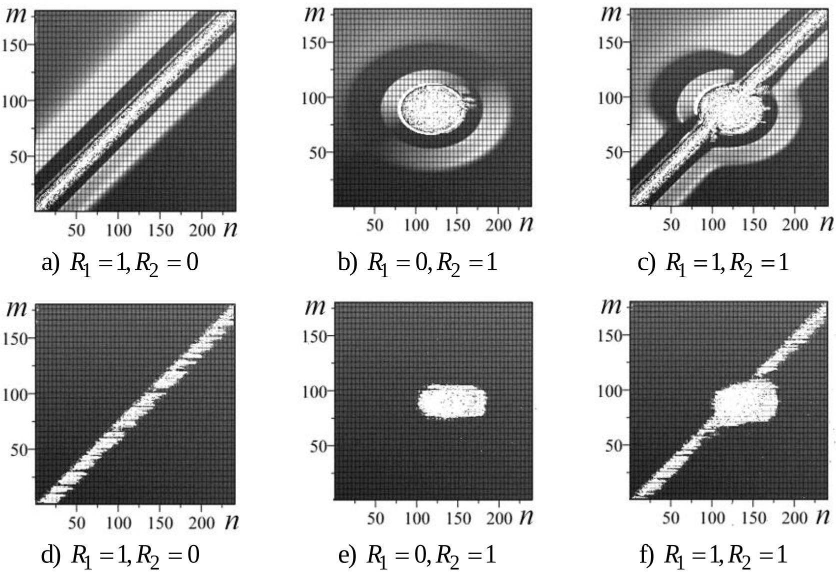

Fig. 3. Cross-sections $\mathrm{Re}(u_1) \in [-0.5; 0.5]$ (a,b,c), $\mathrm{Im}(u_1) \in [-10^{-10}; 10^{-10}]$ (d,e,f) (top view) for dislocation (a,d), quantum dot (b,e), coupled system (c,f) with variable modules k_{i} for u_1 .

The presence of variable modules k_i leads to two branches u_1, u_2 of the solutions of nonlinear equations

$$u_1 = \sum_{i=1}^{2} R_i k_i^2 B_{G1i} ; \quad B_{G1i} = 1 - 2sn^2(u_1 - u_{0i}, k_i) ; \quad k_i^2 = (1-\alpha_i)/Q_i ;$$

$$u_2 = \sum_{i=1}^{2} R_i k_i^2 B_{G2i} ; \quad B_{G2i} = 1 - 2sn^2(u_2 - u_{0i}, k_i') ; \quad k_i' = (1-k_i^2)^{1/2} . \quad (23)$$

The displacement functions u_1 (fig. 3) and u_2 (fig. 4) become complex.
The presence of variable parameters leads to the appearance of the effective damping (fig. 3 d,e,f; 4 d,e,f), the wave behavior (fig. 3 a,b,c; 4 a,b,c) of both the separate dislocations, the quantum dot, and the all coupled system. In this case, the wave behavior, the character of the effective damping for u_1 and u_2 are different.

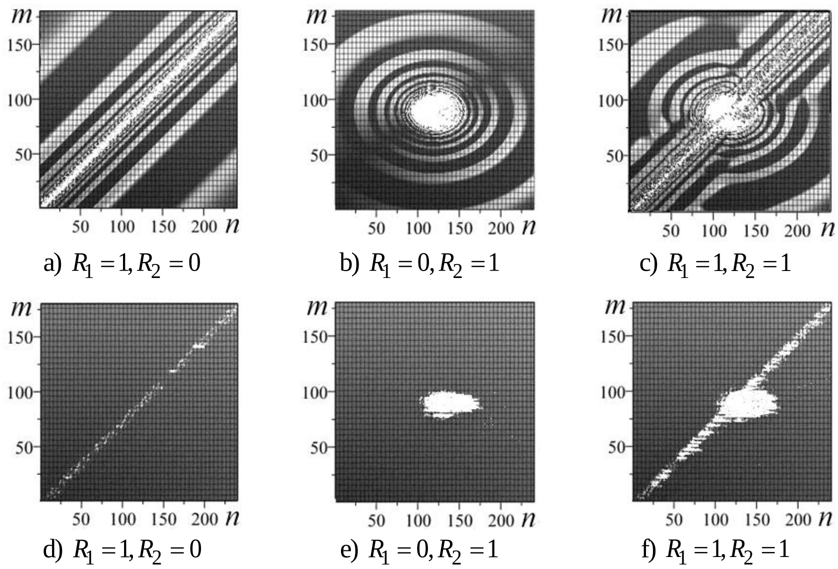

Fig. 4. Cross-sections $\mathrm{Re}(u_2) \in [-0.5; 0.5]$ (a,b,c), $\mathrm{Im}(u_2) \in [-10^{-10}; 10^{-10}]$ (d,e,f) (top view) for dislocation (a,d), quantum dot (b,e), coupled system (c,f) with variable modules k_i for u_2.

The behavior of the deformation field of a coupled system essentially depends on the relationship between the characteristic dimensions $N_1 \times N_2$ of the investigated region and the values of the semi-axes n_{c2}, m_{c2} at the quantum dot (fig. 5). Function u_2 is again complex with pronounced stochastic behavior.

Fractal holes with proportional semi-axes (fig. 5 a), elongated along the axis *On* (fig. 5 b) and along the axis *Om* (fig. 5 c) in elliptical structures are observed inside the region of wave behavior (fig. 5 a,b,c). In this case, a pronounced phenomenon of the anisotropy of the fractal hole appears. The character of the anisotropy for effective damping (fig. 5 d,e,f) agrees with the anisotropy of the fractal hole.

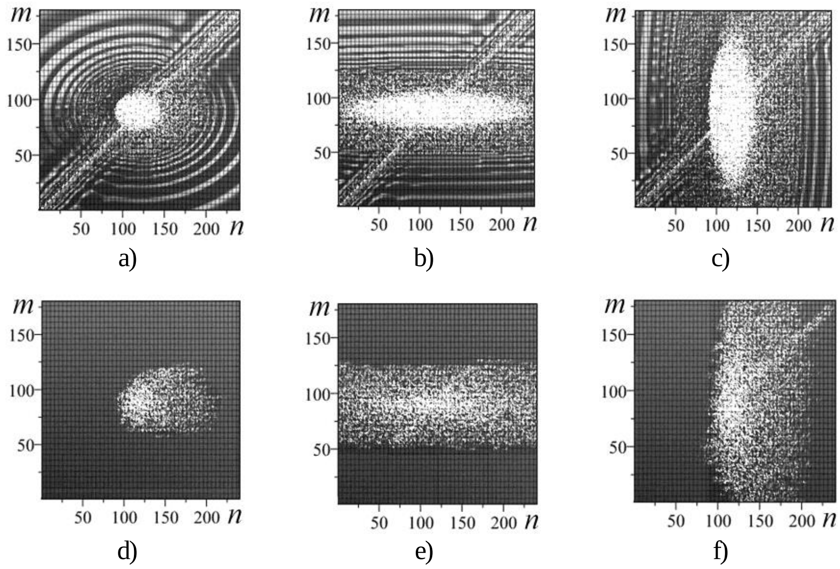

Fig. 5. Cross-sections $\mathrm{Re}(u_2) \in [-10;10]$ (a,b,c), $\mathrm{Im}(u_2) \in [-10;10]$ (d,e,f) (top view) for coupled system with variable modules k_i for u_2 and semi-axes for quantum dot: (a, d) $3n_{c2}$; $3m_{c2}$; (b, e) $12n_{c2}$; $3m_{c2}$; (c, f) $3n_{c2}$; $12m_{c2}$.

Conclusions

Within the framework of **models I** and **II**, the connections between the Hubble constant and the parameters of the Higgs boson are described. It is shown that the inclination angle θ_{H0} of the ecliptic axis to the equator in **model I** is determined through the ratio of the Hubble constant H_{01} and H_{02}. The difference of the inclination angle θ_{E0} in **model II** from θ_{H0} is due to the presence of the parallax of the Sun φ_0.

To describe the relationships between the parameters of the CMB radiation and the Higgs boson **model III** is proposed. Within the framework of this model for variant $V_Q > 0$, $A_Q > 0$ the effect of the accelerated expansion of the Universe is confirmed. Estimates of a number of CMB radiation parameters have been performed. It is shown that the dipole anisotropy appears at $Q_{H3} \neq 0$ (the presence of an inflection point in the functions Q_G, B_Q).

The behavior of the deformation field of a coupled system (dislocation – quantum dot) is investigated within the framework of the fractal model of the Universe. It is shown that the presence of the fractal quantum dot leads to a curvature of the fractal dislocation core. Variable parameters lead to the appearance of the complex displacement functions u. For $\mathrm{Re}(u)$ the wave behavior is characteristic, but $\mathrm{Im}(u)$ leads to an effective damping. The change in the size of the quantum dot leads to a pronounced anisotropy of the deformation field, the change in the structure of the fractal holes.

The obtained results can be used by describing parameters of separate elements of large-scale fractal structures of the Universe (for example, walls, voids), by constructing dynamic models of separate stages formation of the Universe.

References

1. A. Riess et al. Observational Evidence from Supernovae for an Accelerating Universe and a Cosmological Constant. Astronomical Journal, 116,1009{1038, 1998.
2. STARMUS-2016, http://www.starmus.com/tag/starmus-2016-en
3. A. Riess. Explosions of Stars and Expansion of the Universe. Universe, Space, Time, 9,146,4{9, 2016.
4. P.W. Higgs. Broken Symmetries and the Masses of Gauge Bosons. Phys. Rev. Lett., 13,508{509, 1964.
5. B. Greene. String Theory and the Nature of Reality. Universe, Space, Time, 10,147,5{13, 2016.
6. R. Penrose. Fashion, Faith and Fantasy in the New Physics of the Universe. Universe, Space, Time, 11,148,4{10, 2016.
7. S. Hawking. Black Holes and Baby Universes, Transworld Publishers, 1994.
8. B.P. Abbott et al. Observation of Gravitational Waves from a Binary Black Hole Merger. Phys. Rev. Lett., 116, 061102,1{16, 2016.
9. B. Novosyadlyy. Voids - "Deserts" of the Universe. Universe, Space, Time, 6,143,4{11, 2016.
10. V.S. Abramov. The Higgs Boson in Fractal Quantum Systems with Active Nanoelements. Bulletin of the Russian Academy of Sciences. Physics, 80, 7,859{865, 2016.
11. V.S. Abramov. Pairs of Vortex-Antivortex and Higgs Boson in a Fractal Quantum System. CMSIM Journal, 1,3{15, 2017.
12. V.S. Abramov. Quantum dots in the fractal multilayer nanosystem. Bulletin of the Russian Academy of Sciences. Physics, 81, 5,579{586, 2017.
13. O.P. Abramova, A.V. Abramov. Attractors and Deformation Field in the Coupled Fractal Multilayer Nanosystem. CMSIM Journal, 1,16{26, 2017.
14. O.P. Abramova, S.V. Abramov. Governance of Alteration of the Deformation Field of Fractal Quasi-two-dimensional Structures in Nanosystems. CMSIM Journal, 3,367{375, 2013.
15. I.A. Klimishin. Elementary Astronomy, Moscow: Science, 1991.
16. Superfluidity in Helium-3 / Collection of Articles, Moscow: Mir, 1977.